22nd Australasian Fluid Mechanics Conference AFMC2020
Brisbane, Australia, 7–10 December 2020
https://doi.org/10.14264/933c23f

Large-scale spanwise periodicity in a canonical turbulent boundary layer

Rahul Deshpande[1], **Jason P. Monty**[1] **and Ivan Marusic**[1]

[1]Department of Mechanical Engineering, University of Melbourne, Parkville, VIC 3010, Australia

Abstract

The present study reports empirical evidence for periodic organization of very large-scale motions (also known as superstructures), along the spanwise direction, in a zero pressure gradient turbulent boundary layer. This is made possible by performing a scale-specific coherence analysis on datasets comprising streamwise velocity fluctuations, synchronously measured at multiple locations across large spanwise and wall-normal separations within the shear flow. Datasets considered include published low-Re_τ direct numerical simulation and high-Re_τ experimental datasets across a friction Reynolds number range, $Re_\tau \sim O(10^3) - O(10^4)$. The present analysis supports the notion on the superstructures being formed via the streamwise concatenation of relatively smaller motions. The latter are found to exhibit geometric self-similarity over a range of scales, up to a characteristic spanwise width equivalent to that of the superstructures, which scales in outer-units.

Keywords
boundary layer structure; turbulent boundary layers

Introduction

Since the discovery of 'coherent' structures in a wall-bounded turbulent shear flow, a significant number of studies have been conducted to understand the mechanism associated with their formation and organization [13]. One of the earliest efforts in this respect was the seminal work of Kline et al. [7], who observed the near-wall streaky structures to be organized along the spanwise direction, at a characteristic viscous-scaled wavelength of 100, which is common to all three canonical wall-bounded turbulent flows [11] – the zero pressure gradient turbulent boundary layer (ZPG TBL), the fully developed turbulent channel and pipe flow. Studies conducted over the past two decades [14, 3] have reported a similar organization even for the energetic large coherent structures existing in the outer region of the wall-bounded flow, albeit at much larger spacings. The existence of such an 'order within chaos' is particularly exciting from the perspective of developing conceptual models for these complex flows (for example, the attached eddy model based on the attached eddy hypothesis (AEH) of [15]).The present study investigates the organization as well as the geometric characteristics of the energetic motions in a ZPG TBL, in the hope to facilitate the AEH-based modelling for this flow type [9].

Recent modelling efforts have primarily concentrated on the logarithmic (log) region of a wall-bounded shear flow [9], which comprises a major proportion of the turbulence production at practically relevant Reynolds numbers [13]. This region is predominated by the so-called large-scale motions (LSMs;[13]) and very-large-scale motions or superstructures (SS;[6, 11]) carrying streamwise (u) momentum, which together constitute a significant portion of the Reynolds shear stress and turbulent kinetic energy [13] of the flow, making them the primary focus of this study. The LSMs correspond to u-motions with streamwise (x) lengths of the order of 2-3δ, and are induced by hairpin packets formed via coalescence of multiple hairpin vortices along x [13]. δ, here, refers to the boundary layer thickness of a ZPG TBL. Recent direct numerical simulations (DNS) have revealed via space-time analysis [8, 2] that it is these LSMs which concatenate along the streamwise direction to form the SS, an idea earlier hypothesized by [14]. The SS correspond to spanwise-alternatively arranged very long structures ($> 20\delta$) of low ($-u$) and high ($+u$) momentum [6, 11], extending down to the wall (i.e. they are wall-coherent [4]), subsequently influencing the near-wall dynamics via superposition and modulation [6, 10]. While their spanwise periodicity has been noted previously via Fourier analysis [14, 3], these estimates should however, be treated with caution given that the associated wavelengths essentially correspond to Fourier wavelengths [2], which inherently assumes periodicity along the concerned direction.

Consequently, here we re-investigate published datasets, spanning across a decade of Re_τ, to look for a direct evidence of the periodic organization of the SS along the spanwise direction. To this end, experimental and numerical datasets comprising multi-point u-fluctuations measured synchronously across large spanwise (Δy) and wall-normal ($\Delta z = z_o - z_r$) spacings are considered to compute the scale-specific u-coherence over space and/or time. The unique aspect of the present analysis is the consideration of one of the reference u-velocity signals (to investigate coherence) from the near-wall region, which ensures that the estimates are solely influenced by the wall-coherent motions [4, 5]. Given that the SS are formed via concatenation of the LSMs [8, 2], the present analysis also facilitates investigation of these relatively smaller wall-coherent motions acting as the constituent elements for the former. The associated findings would be useful to model the SS, while developing the framework of an AEH-based conceptual model for the ZPG TBL flow [9]. Throughout this article, superscript '+' indicates normalization by viscous length (ν/U_τ) and velocity (U_τ) scales, the latter defined mathematically by $U_\tau = (\frac{\tau_w}{\rho})^{1/2}$, with τ_w and ρ the mean wall-shear stress and fluid density, respectively.

Experimental and numerical data

The flow organization is investigated by conducting a coherence analysis on published datasets ([12, 4]; table 1) ranging over a decade of friction Reynolds number, $Re_\tau \sim O(10^3) - O(10^4)$. Here, $Re_\tau = U_\tau\delta/\nu$, which is the ratio of the inner and outer length scales of the wall-bounded flow. The experimental dataset essentially comprises of the time series of the u-fluctuations (with the mean subtracted from the instantaneous signal) synchronously acquired via hotwire anemometry at multiple locations across the shear flow, specific details of which are given in table 1. The dataset is obtained from one of the largest state-of-the-art facilities available for investigating the ZPG TBL – the Melbourne High Reynolds Number Boundary Layer Wind Tunnel (HRNBLWT) facility at the University of Melbourne. The facility is designed on the 'big and slow' approach, i.e. it allows the TBL to grow along the streamwise direction (x), producing a high Reynolds number flow which is physically thick (meaning a large δ) while keeping the smallest energetic viscous scale within $O(10\,\mu\text{m})$. This permits accessibility to the near-wall region of the high Reynolds number flows, which scales in viscous units, while also ensuring that the entire spectrum of the energetic scales can be resolved by

Study	Deshpande et al. [4]		Sillero et al. [12]	
Facility	HRNBLWT (Exp)		DNS	
$Re_\tau \approx$	14 000		2 000	
Sensor ref.	z_o^+	z_r^+	z_o^+	z_r^+
Location	$2.6\sqrt{Re_\tau}$	$\approx z_o^+$	$2.6\sqrt{Re_\tau}$	$= z_o^+$
Location	$2.6\sqrt{Re_\tau}$, $0.15Re_\tau$	15	$2.6\sqrt{Re_\tau}$	15
$l^+ \approx$	22	22	3.7	3.7
$\Delta s/\delta \approx$	0.0 - 2.5	–	0.0 - 2.5	–

Table 1. A summary of the data sets containing synchronized multipoint u-measurements at z_r^+ and z_o^+, which are separated by various spanwise offsets, Δs. l^+ represents the spatial resolution of the sensor/grid along the spanwise direction. $z_o^+ \approx 2.6\sqrt{Re_\tau}$ and $0.15Re_\tau$ corresponds to the lower and upper bound of the log-region, respectively [4].

conventional hotwire sensors.

In HRNBLWT, the TBL is allowed to develop over a very long flat plate from the start of the test section ($x = 0$), with the multipoint hotwire measurements conducted at $x \approx 20\ m$, where $\delta \approx 0.36\ m$. To facilitate the study of the spanwise organization of the energetic wall-coherent motions, u-fluctuations were acquired simultaneously at locations in the near-wall ($z_r^+ \approx 15$) as well as at the start of the log-region ($z_o^+ \approx 2.6\sqrt{Re_\tau}$). These two probes were separated by a spanwise offset Δs, which was varied by physically traversing the probe at z_o (along the span y) for every measurement while keeping the other probe (at z_r) fixed. Figure 1(a) schematically depicts this probe arrangement. The same experiment was also conducted to investigate the tall wall-coherent motions extending up to the upper bound of the log-region, by choosing $z_o^+ \approx 0.15Re_\tau$, the schematic for which has been given in figure 1(b). The cumulative observations from these two measurements, thus, can be deemed representative of the flow phenomena in the entire log-region.

Apart from the arrangement where $z_o^+ \neq z_r^+ \approx 15$ (table1), a similar two-point measurement but with $z_o^+ \approx z_r^+ \approx 2.6\sqrt{Re_\tau}$ was also conducted to estimate the u-coherence influenced by all motions coexisting at z_o, to compare with the former experiment. Full details of the setup as well as the methodology adopted to conduct both these measurements can be found in [4]. Apart from these experimental data, a low Re_τ dataset of Sillero et al. [12] is also selected from their published DNS database for a ZPG TBL. Thirteen raw DNS volumes, comprising instantaneous streamwise velocity fluctuations, are considered in total to investigate the large-scale coherence. Sensor locations, z_o^+ and z_r^+ for this dataset were selected to be compatible with the experimental dataset and have been specified in table 1.

Results

Here, the spatial coherence of the u-motions is quantified by computing the scale-specific coherence function [1], Γ:

$$\Gamma(z_o, z_r, \Delta s; \lambda_x) = \frac{Re[\langle \widetilde{u}(z_o, \Delta s; \lambda_x)\widetilde{u}^*(z_r; \lambda_x)\rangle]}{\sqrt{\langle |\widetilde{u}(z_o, \Delta s; \lambda_x)|^2\rangle}\sqrt{\langle |\widetilde{u}(z_r; \lambda_x)|^2\rangle}}, \quad (1)$$

where $\tilde{u}(z_o, \Delta s; \lambda_x)$ indicates the Fourier transform of $u(z_o, \Delta s)$ in either time or x, depending on the data set. Here, λ_x is the streamwise wavelength and is equal to $2\pi/k_x$, with k_x the streamwise wavenumber. The asterisk ($*$), angle brackets ($\langle\rangle$) and vertical bars ($||$) indicate the complex conjugate, ensemble averaging in time and modulus, respectively while Re denotes the real component. It is noted, that by definition -1 $\leq \Gamma \leq$ 1, with $+1$ and -1 representing perfect correlation and anti-correlation respectively, analogous to the correlation coefficient which has been widely used in the literature [6, 11] to study spatial coherence. The present study, however, uses Γ as the preferred metric since it allows contributions from the small and large motions to be compared individually, yielding information which is otherwise lost due to ensemble averaging in case of the correlations [1, 5]. It can be noted that, when $z_r^+ \approx 15$, Γ would be solely influenced by the wall-coherent motions [5, 4] at z_o, which is of primary interest to us in this study.

In the case of the experimental dataset, which is limited only to having the u-time series at various Δs, the streamwise coherence in equation 1 is obtained by using the Taylor's frozen turbulence hypothesis, which assumes all large-scale motions to be convecting along x at a common velocity (U_c) throughout the shear flow [1, 13]. Since the present study focuses on investigating the SS in a ZPG TBL, we choose $U_c = 0.75U_\infty$ (where U_∞ is the free-stream velocity) based on their convective velocities estimated in the literature [8].

Large-scale spanwise periodicity

Figure 1 plots the constant energy contours for Γ, as a function of λ_x and Δs scaled with respect to δ, for the high-Re_τ experimental dataset. Here, Γ is estimated for both: $z_o^+ \approx 2.6\sqrt{Re_\tau}$ (figure 1(c)) and $z_o^+ \approx 0.15Re_\tau$ (figure 1(d)), while maintaining $z_r^+ \approx 15$, so that the two plots cumulatively denote scale-specific coherence of the wall-coherent u-motions across the log-region. For discussion, +Γ and -Γ contours are interpreted here as being representative of the statistically averaged +u and -u motions, respectively and are indicated by solid blue and dashed red contours in the plot. High magnitudes for both +Γ and -Γ are seen for small spanwise offsets at large λ_x, which is representative of a +u superstructure flanked on either sides (along y) by a -u superstructure, given the flow symmetry in the spanwise direction. Such an organization is consistent with the observations reported previously in the literature [6, 11, 8].

This arrangement of alternatively arranged very-large-scale u-motions can be noted to be existing even at larger spans, $\Delta s \sim O(\delta)$, albeit represented by relatively weaker contour levels. The low contour levels may be attributed to the fact that the coherence at such large Δs is due to the very large scales [2], which is evident from the positioning of the contours at $\lambda_x \sim O(10\delta)$, corresponding to the SS. The Γ contours in figure 1(c,d), thus, provide direct empirical evidence in support of +u and -u SS statistically organized in a spanwise periodic manner across the log-region of a ZPG TBL. Such a flow organization is brought out only after consideration of the scale-specific coherence over very large spatial offsets, which would be otherwise obscured if the ensemble-averaged correlation coefficient was considered instead. The present interpretation is further substantiated by comparing the centre-to-centre distance between the subsequent peaks (troughs) of +Γ (-Γ) with the dominant spanwise wavelength ($\lambda_y \approx 0.7\delta$) reported in the literature based on Fourier analysis [14, 3]. The two values are consistent across the log-region, as has been highlighted in figure 1(c,d).

Apart from spanwise periodicity, the Γ-contours for the two different z_o^+ also bring out differences in the relatively small-scale contributions ($\lambda_x < 2\delta$), which do not show up in figure 1(d). It signifies that the tall wall-coherent motions are predominantly large in size along both the streamwise and spanwise direction. Figure 1(c), on the other hand, depicts significant coherence in the relatively small λ_x-Δs range at the lower bound of the log-region. Given that the SS are a consequence of the streamwise concatenation of relatively smaller u-motions [8, 2], we now fo-

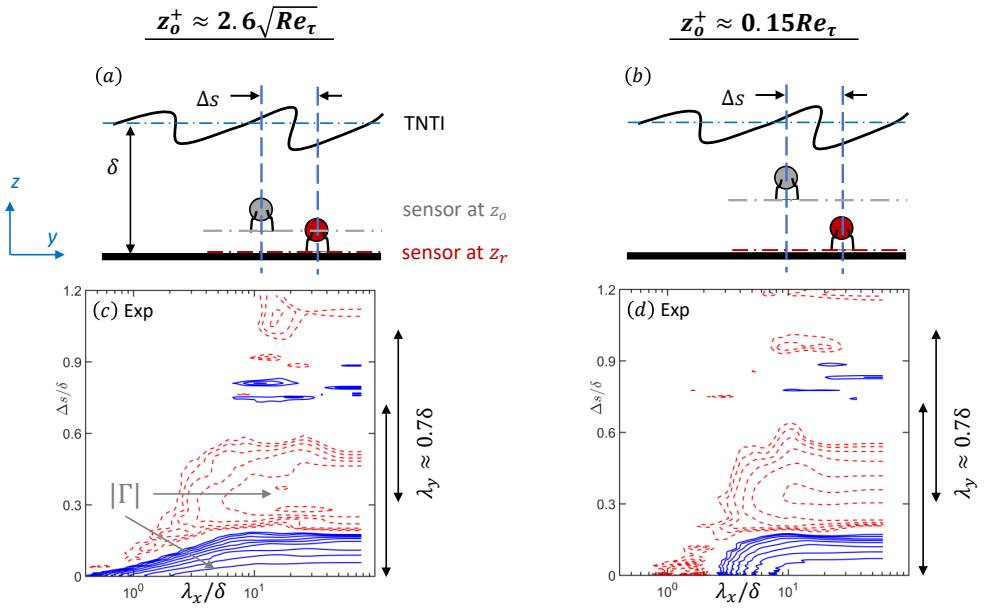

Figure 1. Contours of the coherence function, Γ calculated for the experimental dataset for (c) $z_o^+ \approx 2.6\sqrt{Re_\tau}$, $z_r^+ \approx 15$ and (d) $z_o^+ \approx 0.15Re_\tau$, $z_r^+ \approx 15$, as depicted in the respective schematics of the hotwire setup (a,b). Solid blue and dashed red contours respectively indicate Γ contours with values varying logarithmically in the range (0.05,0.95) and (-0.22,-0.02), in the direction of the arrows shown in (c). The spanwise wavelength estimates (λ_y) denoted in (c,d) correspond to the dominant spanwise Fourier mode noted for the ZPG TBL in the literature [14, 3].

cus on the Γ contours at $z_o^+ \approx 2.6\sqrt{Re_\tau}$, in this λ_x-Δs range, to understand the geometric characteristics of the latter.

Self-similarity of the wall-coherent motions

Figure 2(b,d) depicts Γ contours (with $z_r^+ \approx 15$) for both the experimental and DNS ZPG TBL datasets, with the y-axis plotted on a logarithmic scale to investigate coherence over shorter $\Delta s/\delta$. The contours can be noted to be following the linear trend, $\lambda_x \sim \Delta s$ at spanwise widths $\sim O(0.01\delta)$ for both the datasets, spanning across a decade of Re_τ. This trend is representative of the self-similar variation of the spanwise widths of the wall-coherent u-motions with respect to their streamwise extents (λ_x), consistent with Townsend's AEH [15, 4]. This linear growth, however, ceases at a characteristic width, $W \sim 0.17\delta$, in case of both datasets, which can be described as the average spanwise width of the largest self-similar structure coherent to the wall. Beyond this point, Γ contours vary only along λ_x, suggesting these large self-similar motions as the constituent elements forming the SS, given that their average spanwise widths are equivalent [1]. This can be confirmed by calculating the two-point amplitude modulation coefficient, $\mathcal{R}$, to measure the spanwise extent up to which the wall-coherent SS modulate [6, 10] the small-scales in the near-wall region. To this end, u-time series (from the experimental dataset) synchronously acquired at $z_o^+ \approx 2.6\sqrt{Re_\tau}$ and $z_r^+ \approx 15$ is used to compute $\mathcal{R}$ plotted in figure 2(e) following:

$$\mathcal{R}(z_o, z_r, \Delta s) = \frac{\overline{u_C(z_o, \Delta s; t) E_C(u_I(z_r; t - \Delta t))}}{\sqrt{\overline{u_C^2(z_o, \Delta s)}} \sqrt{\overline{E_C(u_I(z_o, \Delta s))^2}}}, \qquad (2)$$

where subscripts C and I respectively represent filtered u-signals comprising the wavelength range corresponding to the wall-coherent and incoherent scales, while E represents the envelope returned by the Hilbert transform [10]. Overbar indicates the estimate averaged over time, t. The wall-coherent and incoherent components of the u-signal are obtained via the linear coherence spectrum-based procedure described in [5], conducted for the same experimental dataset. To get the maximum correlation in equation (2), a time shift Δt [10] is also applied to the u-signal at z_r to account for the inclination angle of the averaged structure with respect to $u(z_o, \Delta s)$. Interested readers may refer to [5] for complete information regarding the methodology employed to find this inclination angle.

As explained by [10], $\mathcal{R}$ quantifies the intensity with which the SS (at z_o) modulate the near-wall fluctuations, meaning it would drop to zero at $\Delta s/\delta$ extending beyond the average spanwise width of the SS. Interestingly, $\mathcal{R} \to 0$ at the same characteristic width (W) where the Γ contours deviate away from the self-similar trend to grow only along λ_x in figure 2(b,d). This is evidence that the spanwise width of the largest self-similarly grown motions is nominally equal to that of the SS, suggesting the former as the constituent element forming the latter [1, 8, 2]. It should be noted here, that the self-similarity of the intermediate-scaled wall-coherent motions is brought out due to the choice of z_r^+ in the near-wall region (while estimating Γ). For the case of $z_r^+ \approx z_o^+$, which has been plotted in figure 1(a,c), Γ would also be influenced by the wall-incoherent motions at z_o, owing to which the contours no longer follow the linear relationship representative of the self-similarity.

Conclusions

The study investigates the spanwise organization of the energetic large-scale u-motions in a ZPG TBL across a decade of Re_τ. This is facilitated by a scale-specific coherence analysis of the u-fluctuations synchronously acquired over large wall-normal and spanwise spacings across the shear flow. The wall-coherent u-motions in the intermediate-scale range exhibit geometric self-similarity up to a characteristic δ-scaled spanwise width (W), equivalent to that of the SS. A clear evidence of the spanwise periodicity of the SS, which we speculate are formed via the streamwise concatenation of the large self-similar motions, is also reported. The present findings, thus, have direct ramifications towards future AEH-based conceptual modelling of the ZPG TBL flow. The organized state of the energetic

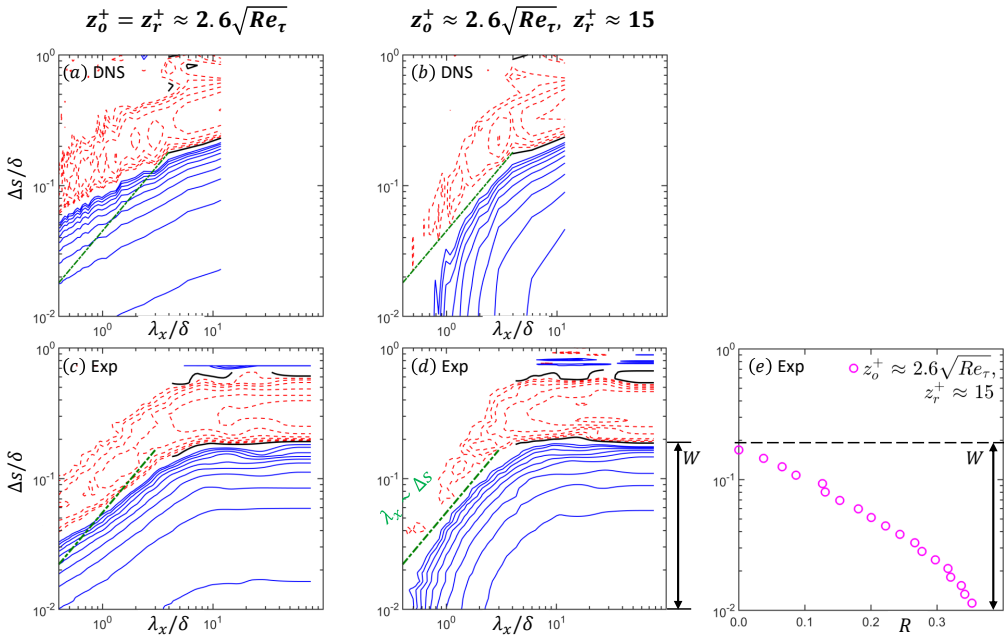

Figure 2. Contours of the coherence function, Γ calculated for the (a,b) DNS and (c,d) experimental datasets for (a,c) $z_o^+ \approx z_r^+ \approx 2.6\sqrt{Re_\tau}$ and (b,d) $z_o^+ \approx 2.6\sqrt{Re_\tau}$, $z_r^+ \approx 15$. Solid blue, dashed red and solid black contours indicate +Γ, –Γ and $\Gamma \approx 0$, respectively while the dash-dotted green line represents the linear relationship, $\lambda_x \sim \Delta s$, representative of the self-similarity. Magnitude of Γ, for both the blue and red contours, increases in the same manner as shown in figure 1 (c,d). (e) Two-point amplitude modulation coefficient ($\mathcal{R}$) calculated from the experimental dataset for various Δs following (2).

large-scale motions, found in the present study, can also facilitate flow-control strategies aimed towards manipulating these motions to achieve drag reduction.

Acknowledgements

The authors wish to acknowledge the Australian Research Council for financial support, and are thankful to the authors of [12] for making their DNS data available.

References

[1] Bailey, S., Hultmark, M., Smits, A. and Schultz, M., Azimuthal structure of turbulence in high Reynolds number pipe flow, *Journal of Fluid Mechanics*, **615**, 2008, 121–138.

[2] Baltzer, J., Adrian, R. and Wu, X., Structural organization of large and very large scales in turbulent pipe flow simulation, *Journal of Fluid Mechanics*, **720**, 2013, 236–279.

[3] de Silva, C. M., Chandran, D., Baidya, R., Hutchins, N. and Marusic, I., Periodicity of large-scale coherence in turbulent boundary layers, *International Journal of Heat and Fluid Flow*, **83**, 2020, 108575.

[4] Deshpande, R., Chandran, D., Monty, J. and Marusic, I., Two-dimensional cross-spectrum of the streamwise velocity in turbulent boundary layers, *Journal of Fluid Mechanics*, **890**, 2020, R2.

[5] Deshpande, R., Monty, J. and Marusic, I., Streamwise inclination angle of large wall-attached structures in turbulent boundary layers, *Journal of Fluid Mechanics*, **877**, 2019, R4.

[6] Hutchins, N. and Marusic, I., Evidence of very long meandering features in the logarithmic region of turbulent boundary layers, *Journal of Fluid Mechanics*, **579**, 2007, 1–28.

[7] Kline, S. J., Reynolds, W. C., Schraub, F. A. and Runstadler, P. W., The structure of turbulent boundary layers, *Journal of Fluid Mechanics*, **30**, 1967, 741–773.

[8] Lee, J. and Sung, H., Very-large-scale motions in a turbulent boundary layer, *Journal of Fluid Mechanics*, **673**, 2011, 80–120.

[9] Marusic, I. and Monty, J. P., Attached eddy model of wall turbulence, *Annual Review of Fluid Mechanics*, **51**, 2019, 49–74.

[10] Mathis, R., Hutchins, N. and Marusic, I., Large-scale amplitude modulation of the small-scale structures in turbulent boundary layers, *Journal of Fluid Mechanics*, **628**, 2009, 311–337.

[11] Monty, J., Hutchins, N., Ng, H., Marusic, I. and Chong, M., A comparison of turbulent pipe, channel and boundary layer flows, *Journal of Fluid Mechanics*, **632**, 2009, 431–442.

[12] Sillero, J. A., Jiménez, J. and Moser, R., Two-point statistics for turbulent boundary layers and channels at Reynolds numbers up to $\delta^+ \approx 2000$, *Physics of Fluids*, **26**, 2014, 105109.

[13] Smits, A., McKeon, B. and Marusic, I., High–Reynolds number wall turbulence, *Annual Review of Fluid Mechanics*, **43**.

[14] Tomkins, C. and Adrian, R., Energetic spanwise modes in the logarithmic layer of a turbulent boundary layer, *Journal of Fluid Mechanics*, **545**, 2005, 141–162.

[15] Townsend, A. A., *The structure of turbulent shear flow*, Cambridge University Press, 1976, 2nd edn. Cambridge University Press edition.